INSTITUT DE FRANCE
Académie des sciences

Comptes Rendus
Géoscience
Sciences de la Planète

Oswaldo Guzmán, Jean-Louis Mugnier, Riccardo Vassallo, Rexhep Koçi, Julien Carcaillet and François Jouanne

Fluvial terrace formation in mountainous areas: (1) Influence of climate changes during the last glacial cycle in Albania

Volume 355 (2023), p. 331-353

Published online: 9 January 2024

https://doi.org/10.5802/crgeos.251

Les Comptes Rendus. Géoscience — Sciences de la Planète *sont membres du Centre Mersenne pour l'édition scientifique ouverte*
www.centre-mersenne.org
e-ISSN : 1778-7025

Comptes Rendus
Géoscience — Sciences de la Planète
2023, Vol. 355, p. 331-353
https://doi.org/10.5802/crgeos.251

Research article — Geomorphology

Fluvial terrace formation in mountainous areas: (1) Influence of climate changes during the last glacial cycle in Albania

Oswaldo Guzmán [a, b], Jean-Louis Mugnier [*, b], Riccardo Vassallo [b], Rexhep Koçi [c], Julien Carcaillet [b] and François Jouanne [b]

[a] Grupo de Investigación en Ciencias de La Tierra y Clima, Universidad Regional Amazónica Ikiam, Muyuna, Ecuador

[b] ISTerre, Université Grenoble Alpes, Université Savoie Mont Blanc, CNRS, IRD, Le Bourget du Lac, France

[c] Institute of Geosciences of the Polytechnical University of Tirana, Albania

E-mail: jemug@univ-smb.fr (J.-L. Mugnier)

Abstract. This work analyses terraces formation from the case of Albanian rivers. An allostratigraphy study of the fluvial terraces is combined with new numerical dating. 30 ^{14}C and 4 ^{10}Be new dated sites along four rivers and 45 ages previously acquired along three other rivers were used to define terrace chronologies at the scale of the whole Albania. Few terrace remnants are related to stages older than the last glacial period and are older than 194 ± 19 ka. Terrace level (T1) includes plain-like terraces and T1 is related to a rapid succession of valley incision and valley fill that occurred during the warm Holocene climatic optimum. The other nine terrace levels (T2 to T10) formed during the last glacial period (MIS 5d to end of MIS 2). Terraces T2, T6 and T7 formed nearly synchronously with interstadial transitions toward warmer and wetter conditions. The formation of terraces T3, T4, T5 and T8 (<60 ka) coincide with the warm climatic excursions of the Heinrich events. This result suggests that these short climatic events strongly punctuate the geomorphologic dynamics of rivers in mountainous areas.

Keywords. Fluvial sedimentation, Climatic and vegetation controls, River piracy, Late glacial cycle, Interstadials, *In situ* produced ^{10}Be dating, ^{14}C dating.

Funding. NATO SFP 977993 and the Science for Peace team, Institut de Recherche et Developement.

Manuscript received 22 September 2023, revised 9 December 2023, accepted 13 December 2023.

1. Introduction

A huge body of published works [e.g. see the bibliography in Cordier et al., 2017] suggests that the formation of river terraces, defined as flat surfaces above fluvial sediment, is affected by climate. It has been demonstrated that, in general, river incision took place at climatic transitions [e.g. Vandenberghe, 2003, 2015, Bridgland and Westaway, 2008, Antoine et al., 2016]. Nonetheless, numerous studies show that terraces are not a simple climatic proxy [Cordier et al., 2017, Schanz et al., 2018, Pazzaglia, 2022] and numerous processes interact together in terrace

* Corresponding author.

formation [Starkel, 1994, Vandenberghe, 2003, 2015]. Furthermore, it has been stressed that climatic variations must cross thresholds of duration or magnitude to induce changes between erosion and deposition [e.g. Schumm, 1979, Vandenberghe, 2003]. The role of the succession of the glacial/interglacial periods is classically described for major fluctuations at 10^5 years scale [e.g. Starkel, 1994, Riser, 1999]. However, the role of shorter time scale climatic fluctuations is frequently discussed from the compilation of geochronologic studies distributed on very large areas [Pazzaglia, 2022] but is usually poorly evidenced along single rivers [Woodward et al., 2008].

Terrace levels, formed during the last glacial cycle, are widely preserved along all the Albanian rivers [Woodward et al., 2008, Carcaillet et al., 2009, Koçi et al., 2018]. Albanian river catchments (Figure 1) are located in an area where large-scale controls (climate, tectonics or eustatism) can be considered similar: the climate is Mediterranean [Ozenda, 1975], the tectonics is controlled by the Adriatic subduction beneath southeastern Europe [Roure et al., 2004] and all rivers have the same base level fluctuations linked to the eustatism [Lambeck and Chappell, 2001].

Many studies have already described the general morphology of terraces [Melo, 1961, Prifti, 1981, 1984, Prifti and Meçaj, 1987, Lewin et al., 1991, Woodward et al., 2008] and other studies have focused on the history of incision/uplift [Carcaillet et al., 2009, Guzmán et al., 2013, Gemignani et al., 2022]. But to make progress in understanding the genesis of terraces, numerical chronological constraints are necessary and are therefore proposed in this article.

There was few ages for the river terraces preserved in the central and northern part of Albania. Four ^{10}Be and 21 ^{14}C new terrace ages, as well as geomorphological data, are reported in this paper. These data are combined with previous results in order to furnish an allostratigraphic/chronologic framework for the unit deposition and terrace formation during the past 200 ka along 7 Albanian rivers. This enriched database supported by 70 numerical ages is used to discuss the influence of climate changes on the genesis of terraces.

2. Methodology

Field surveys have been performed along all the rivers and the allostratigraphic units [Hughes, 2010] were defined from an analysis of the lithostratigraphy and the geometry of the interface between Quaternary sediment and bedrock. Thicknesses and characteristics of the sedimentary units were observed in approximately one thousand sites. The terrace extension at large scale was mapped on the basis of field observations reported on topographic maps at the 1:25,000 scale [Institutin Topografik te Ushtrise Tirana, 1990], 30-m digital elevation models [SRTM, 2013] and satellite images (image@2023CNES/Airbus, available on Google Earth).

2.1. *Dating of sedimentary units and terrace surfaces*

In a first step, the relative chronology of the terraces was deduced for each river from the geometric relationship between the mapped terraces [Prifti, 1981, 1984, Prifti and Meçaj, 1987]. The correlation between the terrace remnants was performed by reconstructing a regular paleo-river profile from the upstream to downstream zones [Guzmán et al., 2013].

Although some relative methods, such as those based on the soil chronosequence, can differentiate the age of Middle Pleistocene sequences [Rowey and Siemens, 2021], they were not used in this work: in the studied area, a dozen levels of terraces are distributed over a time period spanning one hundred thousand years [Carcaillet et al., 2009], a temporal distribution not favorable to the use of surface alteration as a time indicator [Rixhon, 2022]. Furthermore, it has been shown that numeric dating is the best way to compare terrace chronologies at a large scale [Woodward et al., 2008] and that absolute dating techniques are necessary to correlate terraces with climatic stages [Schaller et al., 2016].

In a second step, the numeric ages of the terraces were determined. New data were based on radiocarbon (^{14}C) and *in situ* produced ^{10}Be dating. (See Supplementary Information, Appendix 1 and Appendix 2 for technical details.)

The ^{14}C ages represent the death of organic material. Samples consist of plant remains or charcoal, a few millimeters in size (Supplementary Information, Figure S1b in Appendix 1), which are transported rapidly by rivers. Although there may be a delay between plant death and final deposition, we consider ^{14}C ages to represent the age of sediment deposition. In order to exclude an eolian origin,

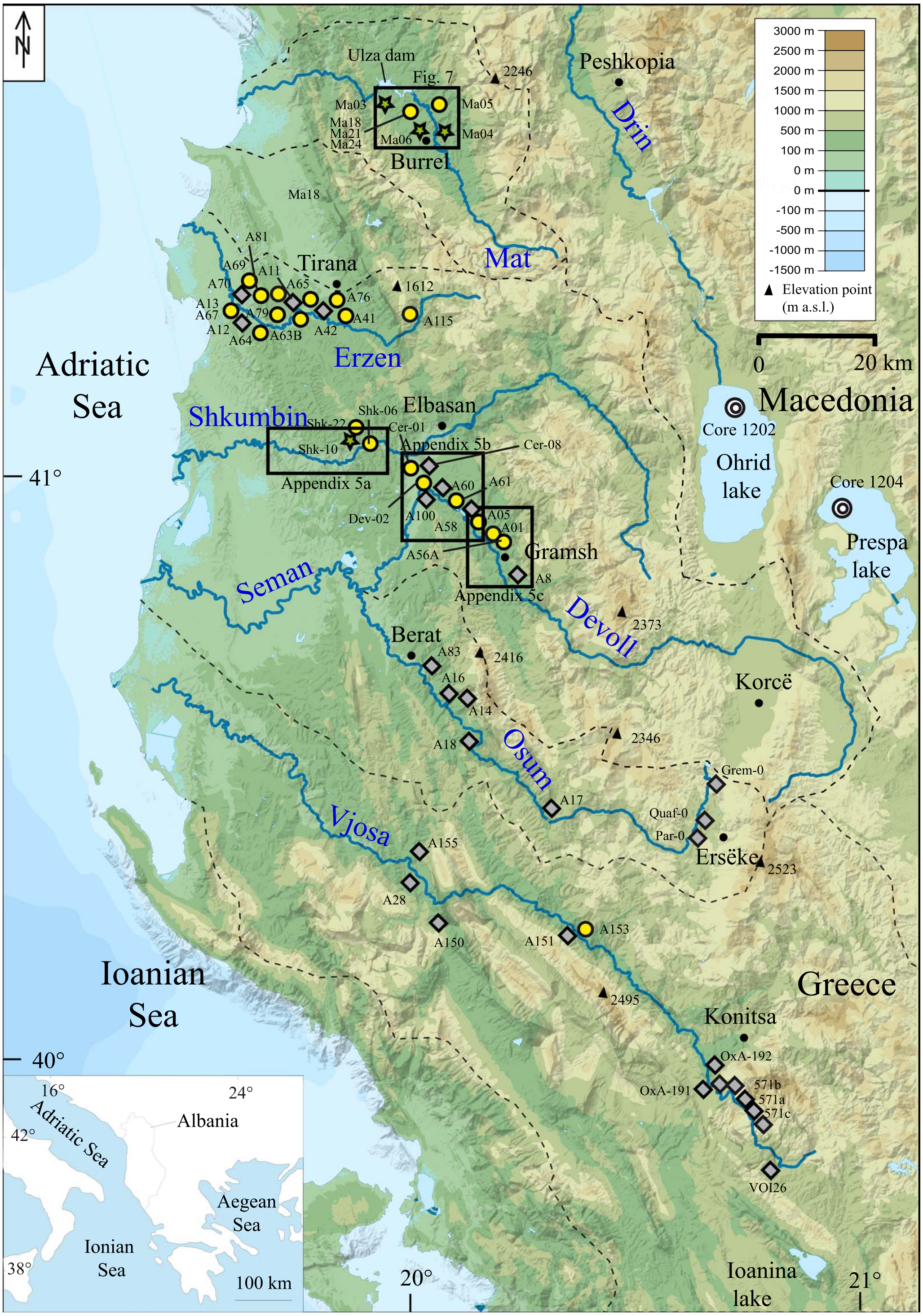

Figure 1. Caption continued on next page.

Figure 1. (**cont**.) The rivers of Albania. (a) Topographic map of Albania derived from the 90-m Shuttle Radar Topography Mission (SRTM) digital elevation model. Watersheds of the seven main Albanian rivers are bounded by black dashed lines. Dark diamonds indicate published data [Lewin et al., 1991, Hamlin et al., 2000, Woodward et al., 2001, 2008, Carcaillet et al., 2009, Guzmán et al., 2013, Koçi et al., 2018], yellow circles (^{14}C dating) and green stars (^{10}Be dating) indicate the data obtained in this study. The boxes show the location of Supplementary Information, Appendix 5 and Figure 7. Core 1202 and 1204 in the Ohrid and Prespa lakes refer to the work of Wagner et al. [2009, 2010, see Figure 9].

that has sometimes been suggested in the Mediterranean area for the formation of the upper subunit of fine-grained deposits [Woodward et al., 2008, Obreht et al., 2014, Cremaschi et al., 2015], the samples were taken from deposits also containing some coarse sands and small gravels or from fine-grained lenses within the coarse material (Supplementary Information, Figure S1c, Appendix 1). Therefore most ^{14}C samples were collected close to the bottom of the upper sub-unit (see Supplementary Information, Figure S1a, Appendix 1).

The ^{10}Be ages represent the exposure ages of the terrace surfaces [Gosse and Phillips, 2001]. The ^{10}Be concentration on the terrace surface was measured in samples formed of amalgamated quartz clasts less than 5 cm in length. The attenuation of ^{10}Be at depth was analysed by sampling cobble samples along one profile and amalgamated pebbles samples along another one [Gosse and Phillips, 2001]; the best fit profiles and their uncertainties were then calculated using a Monte Carlo approach [Hidy et al., 2010] (Table 1). In addition to the new ^{10}Be ages, the previously published ^{10}Be ages were re-calibrated following the same procedure (Table 2).

The limestone pebble-rich terraces of the Drin River [Gemignani et al., 2022] have been dated using ^{36}Cl. Other ages [Lewin et al., 1991, Woodward et al., 2008] refer to the mineral formation (U/Th) or the time without daylight exposure (ESR and TL) within the alluvium and are older than the ultimate phases of river aggradation [Noller et al., 2000].

3. Setting

3.1. *Climate and paleoclimate of Albania*

Albania's present climate is Mediterranean on the coast, with 2 to 3 hot, dry months in summer and 4 to 5 mild, rainy months in winter. In the mountainous regions, the climate is continental with cold and snow-covered winters.

The paleo climatic records for the last 500 ka were studied in the region in Lake Ohrid, [Sadori et al., 2016] and Lake Ioannina [Roucoux et al., 2008] (location on Figure 1). These local records correspond well with the results found in the isotope record of Greenland [Grootes et al., 1993] or in the marine records of the Iberian margin [de Abreu et al., 2003] and the eastern Mediterranean [Konijnendijk et al., 2015]. They show a succession of cold periods followed by rapid warm excursions [Clement and Peterson, 2008].

The Adriatic Sea, which controls the base level of Albania's rivers, was affected by eustatic fluctuations which are tuned to the global sea level variations and ranged from −120 m to +10 m during the last glacial period [Lambeck and Chappell, 2001]. Colder sea surface temperatures that occurred in the Mediterranean Sea [Cacho et al., 1999, Sánchez Goñi et al., 2002, Geraga et al., 2005] during Marine Isotope Stages (MIS) 5 to 2 were linked to the polar water that entered through the Strait of Gibraltar and were closely related to ice rafting events in the northeast Atlantic, called Heinrich events (HEs) [Heinrich, 1988]. These short cold events [one to two thousand years; Chappell, 2002, Ziemen et al., 2019] or even less [Bond et al., 1992, Hemming, 2004] were always followed by warm periods [Rahmstorf, 2002]. Therefore, the temperature evolution of the Albanian region at the millennial scale is similar to that of the north Atlantic domain [e.g. Sánchez Goñi et al., 2002, Tzedakis et al., 2004].

The climatic-water-balance of the landscape (ratio between rainfall, runoff, evapotranspiration, etc.) induces complex connection between temperature and precipitation within the region and a decline in precipitation probably occurred in the western Mediterranean Sea during the Heinrich events. They induced cooler sea surface temperatures that inhibited the moisture supply to the atmosphere [Kallel et al., 1997, 2000] whereas increased rainfalls in the western Mediterranean region are evidenced

Table 1. Results of the ^{10}Be analysis (see Figure 6 and the Supplementary Information, Appendix 2)

Sample	Type of sample	Lithology	Latitude (° N)	Longitude (° E)	Altitude (m)	Depth (cm)	Shielding factor	^{10}Be concentration (10^5 at/g)	^{10}Be age (ka)	Terrace
Lower paleo-Devoll										
Shk-10	Cobble	Quarzite	41.0618	19.8685	65	30	0.998	0.77 ± 0.07	18.81 ± 2.4	$T3_{(pa)}$
Shk-11	Cobble	Granite				47		0.21 ± 0.05		
Shk-12	Amalgam.pebbles	Heterogeneous				75		0.61 ± 0.03		
Shk-14	Cobble	Granite				157		0.47 ± 0.06		
Shk-16	Cobble	Granite				240		0.66 ± 0.05		
Mat river-Uzal Dam										
Ma-03	Amalgam.pebbles	Heterogeneous	41.6748	19.9166	183	10	0.998	4.40 ± 0.14	100.8 ± 9.4	$T8_{(ma)}$
Ma-09	Amalgam.pebbles	Heterogeneous				285		0.52 ± 0.06		
Ma-08	Amalgam.pebbles	Heterogeneous				495		0.27 ± 0.02		
Ma-07	Amalgam.pebbles	Heterogeneous				590		0.26 ± 0.01		
Mat river-Livadhi										
Ma-04	Amalgam.pebbles	Heterogeneous	41.5920	20.0336	262	0	1	5.63 ± 0.16	$\geq 112.32 \pm 10.3$	$T8_{(ma)}$
Mat river-Burrel										
Ma-06	Amalgam.pebbles	Heterogeneous	41.6042	20.0130	322	0	1	10.04 ± 0.40	$\geq 193.92 \pm 19.3$	$T9_{(ma)}$

The depth profiles are from $T3_{(pa)}$ and $T8_{(ma)}$ (location of Shk-10 and Ma-03 on the Supplementary Information, Appendix 5 and Figure 7, respectively). Samples Ma-04 and Ma-06 are amalgamated clasts collected at the top surface of terraces $T8_{(ma)}$ and $T9_{(ma)}$, respectively (location on Figure 7).

Table 2. Numeric ages from fluvial terraces of Albania

Sample[a]	[b]	Latitude (° N)[c]	Long. (° E)[c]	Sample elevation above the river (m)	Sample depth below the surface (m)	Method[d]	Lab-code reactor reference	^{14}C ages (ka)	Calibrated interval ^{14}C Cal ka BP (Probability = 0.95)	Ages (ka)[e]	Local terrace name	Regional terrace name	Source[f]
Vjosa													
A153	C	40.2076	20.3875	17.3	0.7	^{14}C	SacA 16001	190 ± 30	32–302	-	-	colluv.	This study
A150	C	40.2084	20.0934	9.5	0.5	^{14}C	SacA 15998	330 ± 30	308–473	-	-	colluv.	(1)
A28	Vd	40.3354	19.9921	12	2	^{14}C	Poz-8824	705 ± 30	565–691	-	-	colluv.	(1)
OxA-192	C	39.97(ç)	20.66(ç)	~4.5	<1	^{14}C	OxA-192	800 ± 100	560–928	-	$T1_{(vj)}$	T0	(3)
OxA-191	C	40.87(ç)	21.65(ç)	~4.5	<1	^{14}C	OxA-191	1000 ± 50	789–1049	-	$T1_{(vj)}$	T0	(3)
A155	Vd	40.3611	19.9907	13.4	4	^{14}C	SacA 16002	3870 ± 60	4094–4436	-	-	colluv.	(1)
OxA-5246	C	39.96(ç)	20.65(ç)	~10.6	~0.1	^{14}C	OxA-5246	13810 ± 130	16,291–17,116	-	$T3_{(vj)}$	T3	(4)
Beta-109162	C	39.96(ç)	20.65(ç)	~10.6	~0.1	^{14}C	Beta-109162	13960 ± 260	16,203–17,647	-	$T3_{(vj)}$	T3	(4)
Beta-109187	C	39.96(ç)	20.65(ç)	~10.4	~0.4	^{14}C	Beta-109187	14310 ± 200	16,865–17,947	-	$T3_{(vj)}$	T3	(4)
VOI24	S	39.94(ç)	20.71(ç)	~9.7	<1	TL	VOI24	-	-	19.60 ± 3.00	$T3_{(vj)}$	T3	(3)
Tributary site	Cc	39.95(ç)	20.68(ç)	~10.5	~1.6	U/Th	-	-	-	21.25 ± 2.50	$T3_{(vj)}$	T3	(5)
Old Klithonia	Cc	39.96(ç)	20.65(ç)	~9.3	~2.3	U/Th	-	-	-	24.00 ± 2.00	$T4_{(vj)}$	T4	(5)
571c	Dt	39.96(ç)	20.68(ç)	~12.4	~7.5	ESR	571c	-	-	24.30 ± 2.60	$T4_{(vj)}$	T4	(3)
571a	Dt	39.96(ç)	20.68(ç)	~12.4	~7.5	ESR	571a	-	-	25.00 ± 0.50	$T4_{(vj)}$	T4	(3)
Old Klithonia	Cc	39.96(ç)	20.65(ç)	~9.3	~5	U/Th	-	-	-	25.00 ± 2.00	$T4_{(vj)}$	T4	(5)
571b	Dt	39.96(ç)	20.68(ç)	~12.4	~7.5	ESR	571b	-	-	26.00 ± 1.90	$T4_{(vj)}$	T4	(3)
VOI23	S	39.96(ç)	20.68(ç)	~12.4	<1	TL	VOI23	-	-	28.00 ± 7.10 (£)	$T4_{(vj)}$	T4	(3)
A151	C	40.2140	20.3842	21.7	0.3	^{14}C	SacA 15999	24070 ± 150	27,783–28,848	-	$T5_{(vj)}$	T5	This study
Konitsa1	Cc	39.86(ç)	20.77(ç)	~10	~1–1.5	U/Th	-	-	-	53.00 ± 4.00	$T6_{(vj)}$	T8	(5)
Konitsa2	Cc	39.86(ç)	20.77(ç)	~10	~1-1.5	U/Th	-	-	-	56.50 ± 5.00	$T6_{(vj)}$	T8	(5)
Konitsa3	Cc	39.86(ç)	20.77(ç)	~11	~1–1.5	U/Th	-	-	-	74.00 ± 6.00	$T7_{(vj)}$	T9	(5)
Konitsa4	Cc	39.86(ç)	20.77(ç)	~12.7	~1–1.5	U/Th	-	-	-	80.00 ± 7.00	$T7_{(vj)}$	T9	(5)
Konitsa5	Cc	39.86(ç)	20.77(ç)	~15.5	~1–1.5	U/Th	-	-	-	113.00 ± 6.00	$T8_{(vj)}$	T10	(5)
VOI26	S	39.86(ç)	20.77(ç)	~56	~22	TL	VOI26	-	-	>150(£)	$T9_{(vj)}$	T12	(3)

(continued on next page)

Table 2. (continued)

Sample[a]	[b]	Latitude (° N)[c]	Long. (° E)[c]	Sample elevation above the river (m)	Sample depth below the surface (m)	Method[d]	Lab-code reactor reference	^{14}C ages (ka)	Calibrated interval ^{14}C Cal ka BP (Probability = 0.95)	Ages (ka)[e]	Local terrace name	Regional terrace name	Source[f]
Osum													
A17	Vd	40.4508	20.2808	17	2	^{14}C	Poz-10576	9990 ± 50	11,263–11,705	-	$T2_{(os)}$	T2	(2)
Par-0 (*)	Sr	40.5200	20.7200	70	0	^{10}Be	-	-	-	19.25 ± 1.3	$T3_{(os)}$	T3	(2)
Quaf-0 (*)	Sr	40.5500	20.6900	29	0	^{10}Be	-	-	-	20.33 ± 1.5	$T3_{(os)}$	T3	(2)
A16	Vd	40.6394	20.0553	24	4	^{14}C	Poz-10575	29900 ± 1300	31,323–37,457	-	$T5_{(os)}$	T6	(2)
A83	C	40.6800	20.0200	14.8	3.7	^{14}C	Poz-13850	37000 ± 300	41,036–42,066	-	$T6_{(os)}$	T7	(2)
A18	Vd	40.5600	20.1400	53	6	^{14}C	Poz-10578	45300 ± 1600	>46237	50.70 ± 1.80 ($)	$T7_{(os)}$	T8	(2)
A14	Vd	40.6403	20.0575	33.8	1.2	^{14}C	Poz-10574	49000 ± 2500	>49928	54.40 ± 2.78 ($)	$T7_{(os)}$	T8	(2)
Grem-0(*)	Sr	40.5560	20.7383	50	0	^{10}Be	-	-	-	54.01 ± 3.0	$T7_{(os)}$	T8	(2)
Paleo-Devoll													
A05	Vd	40.9092	20.1393	34	2	^{14}C	Poz-10572	119.5 ± 0.3 pMC	-	modern	-	colluv.	This study
Cer-08	C	41.0275	19.9817	8.4	0.6	^{14}C	Poz-39495	30 ± 80	9–275	-	-	colluv.	(1)
Dev-02	C	40.9910	20.0165	16.6	0.5	^{14}C	Poz-39496	540 ± 130	306–727	-	-	colluv.	(1)
Shk-06	Vd	41.0663	19.8800	52.8	2.2	^{14}C	Poz-34987	162 ± 0.46 pMC		modern	-	colluv.	This study
Shk-22	C	41.0649	19.8714	6.3	0.7	^{14}C	Poz-39201	90 ± 30	22–266	-	-	colluv.	This study
Cer-01	C	41.0100	20.0083	8.4	1.6	^{14}C	Poz-39197	5400 ± 40	6021–6293	-	$T2_{(pa)}$	T1	This study
Shk-10(*)	Sr	41.0618	19.8685	14.7	0.3	^{10}Be	-	-		18.81 ± 2.4	$T3_{(pa)}$	T3	This study
A60	C	40.9676	20.0526	19	0.5	^{14}C	Poz-12223	17640 ± 160	20,895–21,800	-	$T3_{(pa)}$	T3	(1)
A58	C	40.9214	20.1292	15.7	3	^{14}C	Poz-12116	21850 ± 150	25,815–26,437	-	$T4_{(pa)}$	T4	(1)
A100	C	40.9660	20.0636	24	1	^{14}C	Poz-17242	22780 ± 200	26,583–27,490	-	$T4_{(pa)}$	T4	(1)
A8	Vd	40.8271	20.2154	42.5	5	^{14}C	Poz-9838	23760 ± 150	27,580–28,163	-	$T5_{(pa)}$	T5	(1)
A1	Vd	40.8836	20.1773	42	6	^{14}C	Poz-8816	25500 ± 300	28,921–30,498	-	$T5_{(pa)}$	T5	This study
A61	C	40.9414	20.1089	41.2	1	^{14}C	Poz-12117	38900 ± 700	41,939–44,142	-	$T7_{(pa)}$	T7	This study
A56A	C	40.8834	20.1764	41	3	^{14}C		>52000		>52	$T8_{(pa)}$	T8	This study
Erzen													
A41	C	41.2697	19.8400	3	1.5	^{14}C	Poz-8826	170 ± 30	35–291	-	-	colluv.	(6)
A11	C	41.2900	19.7100	3.4	0.8	^{14}C	Poz-8818	200 ± 30	25–304	-	-	colluv.	(6)
A81	C	41.2866	19.7094	23.4	1	^{14}C	Poz-13849	275 ± 35	152–459	-	-	colluv.	This study
A65	C	41.3088	19.7544	29	0.8	^{14}C	Poz-12784	500 ± 30	501–617	-	-	colluv.	This study
A76	Vd	41.2800	19.8300	11.7	1	^{14}C	Poz-13847	3075 ± 35	3182–3372	-	-	colluv.	This study

(continued on next page)

Table 2. (continued)

Sample[a]	[b]	Latitude (° N)[c]	Long. (° E)[c]	Sample elevation above the river (m)	Sample depth below the surface (m)	Method[d]	Lab-code reactor reference	^{14}C ages (ka)	Calibrated interval ^{14}C Cal ka BP (Probability = 0.95)	Ages (ka)[e]	Local terrace name	Regional terrace name	Source[f]
A63B	C	41.2870	19.7197	17	3	^{14}C	Poz-12118	3700 ± 35	3927–4150	-	-	colluv.	This study
A13	C	41.2700	19.6400	9	0.4	^{14}C	Poz-8823	1660 ± 30	1421–1690	-	$T1_{(er)}$	T0	(6)
A12	C	41.2700	19.6400	9	1	^{14}C	Poz-10573	1730 ± 30	1564–1708	-	$T1_{(er)}$	T0	This study
A42	Vd	41.2700	19.8000	12	1	^{14}C	Poz-8827	6840 ± 60	7578–7817	-	$T2_{(er)}$	T1	(6)
A115	C	41.2844	19.9683	17	0.8	^{14}C	Poz-17243	26600 ± 500	29,631–31,465	-	$T3_{(er)}$	T5	This study
A67	C	41.2700	19.6400	9.4	3	^{14}C	Poz-12120	30400 ± 300	33,889–34,912	-	$T4_{(er)}$	T6	This study
A69	C	41.2900	19.6400	41	1.2	^{14}C	Poz-12121	31500 ± 400	34,671–36,231	-	$T4_{(er)}$	T6	(6)
A64	C	41.2700	19.7100	24.8	0.8	^{14}C	Poz-12224	33400 ± 500	36,358–38,827	-	$T4_{(er)}$	T6	This study
A79	C	41.2900	19.7100	26.5	2	^{14}C	Poz-13848	44200 ± 1600	>45447	49.59 ± 1.76($)	$T6_{(er)}$	T8	This study
A70	C	41.2900	19.6000	22	0.5	^{14}C	Poz-12785	48000 ± 2000	>49910	53.40 ± 2.22($)	$T6_{(er)}$	T8	(6)
Mat													
Ma-05	C	41.6178	20.0294	24.3	0.7	^{14}C	Poz-34984	1075 ± 30	931–1056	-	-	colluv.	This study
Ma-18	C	41.6245	19.9978	7	0.7	^{14}C	Poz-39198	1725 ± 30	1562–1706	-	$T1_{(ma)}$	T0	This study
Ma-21	C	41.6246	19.9970	10.3	0.7	^{14}C	Poz-39199	5100 ± 40	5746–5922	-	$T2_{(ma)}$	T1	This study
Ma-24	C	41.6273	19.9968	26	2.1	^{14}C	Poz-39200	14850 ± 80	17,856–18,296	-	$T3_{(ma)}$	T3	This study
Ma-04(*)	Sr	41.5920	20.0336	100	0	^{10}Be	-	-	-	100.8 ± 9.4	$T8_{(ma)}$	T10	This study
Ma-03	Sr	41.6748	19.9166	94	0.1	^{10}Be	-	-	-	≥ 112.32 ± 10.3	$T8_{(ma)}$	T10	This study
Ma-06	Sr	41.6042	20.0130	190	0	^{10}Be	-	-	-	≥ 193.92 ± 19.3	$T9_{(ma)}$	T11	This study
Drin													
TPN(*)	Ca	42.37855	20.08971	12	0.5	^{36}Cl	-	-	-	8.2 (−2/ + 4)	$T2_{(dr)}$	T1	(7)
TPS(*)	Ca	42.34380	20.11545	56	0.4	^{36}Cl	-	-	-	12.3 (−2/ + 5)	$T3_{(dr)}$	T2	(7)

[a]Samples: (*) for a cosmogenic depth profile, only the age of the surface and the depth of the shallowest sample are given. [b]Type of material dated: C = charcoal, Vd = vegetal debris, Cc = calcite cement, S = sediment, Dt = deer tooth, Sr = siliceous rock, Ca = Calcereous rock. [c]Location from GPS coordinates or (ç) estimated from published maps. [d]Dating method: ^{14}C = radiocarbon, TL = thermoluminescence, U/Th = uranium series, ESR = electron spin resonance, ^{10}Be and ^{36}Cl = cosmogenic in situ produced data. [e]Numerical ages: all ^{10}Be ages have been calculated (Table 1) or recalculated with the parameters indicated in Supplementary Information, Appendix 2. All ^{14}C ages have been estimated from the IntCal 13 calibrated intervals and the oldest ($) were also corrected using the polynomial calibration of Bard et al. [2004]. (£) Have not been considered for the probability density curves due to their large uncertainty.
[f]Source: (1) Guzmán et al. [2013], (2) Carcaillet et al. [2009], (3) Lewin et al. [1991], (4) Woodward et al. [2008], (5) Hamlin et al. [2000], (6) Koçi et al. [2018], (7) Gemignani et al. [2022].

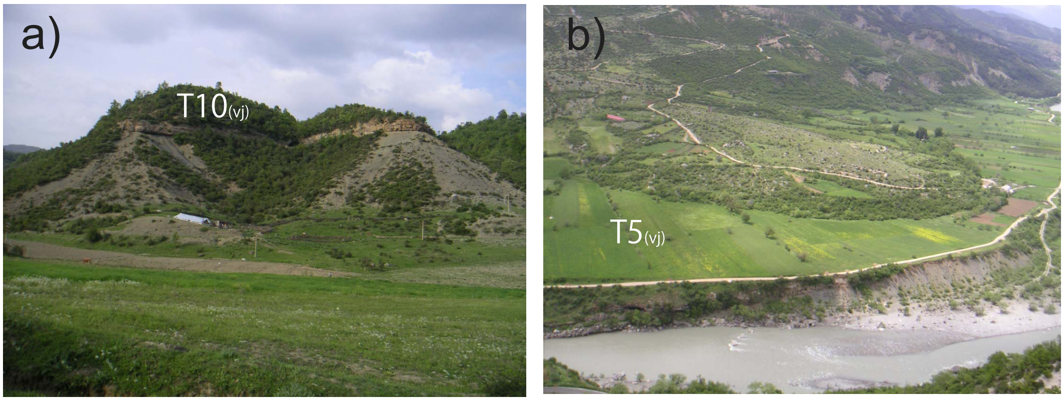

Figure 2. Examples of sedimentary units and terraces in Albania. (a) Remnant of a fill terrace ($T10_{(vj)}$), middle section of the Vjosa River; (b) Debris flow deposited above $T5_{(vj)}$ terrace.

during warm intervals by the sapropel records [Toucanne et al., 2015].

Thus, it is expected that high-frequency Heinrich events induced rapid climatic changes in the Mediterranean region with a succession of dry and cold events followed by rapid warming and moisture return [Toucanne et al., 2015]. Lacustrine sediments in eastern Albania also recorded HEs-induced climatic changes through proxies of the alteration, like a high concentration of manganese and total inorganic carbon [Wagner et al., 2010] and a high zirconium/titanium ratio [Wagner et al., 2009].

3.2. *Geology and rivers of Albania*

The Albanian mountains are parts of the fold belt, which was thrusted westward during the subduction of the Adriatic plate beneath southeastern Europe [Roure et al., 2004]. The eastern side of Albanides mainly consists of Jurassic ophiolites and Mesozoic carbonates. The western side of Albanides is mainly formed of carbonates topped by Mesozoic or Cenozoic flysch deposits [Robertson and Shallo, 2000]. A foreland basin, filled with Plio-Quaternary molasse deposits, forms the coastal plain [Roure et al., 2004].

The late Pleistocene uplift rate, inferred from fluvial incision, locally reaches 2.8 mm/yr in the Albanian mountain but is generally in the range 0.5 to 1.0 mm/yr [Carcaillet et al., 2009, Guzmán et al., 2013, Biermanns et al., 2018]. Permanent GPS stations indicate the same range of values for the present-day vertical motion in Albania (Jouanne, personal communication).

The main Albanian rivers are, from south to north, the Vjosa, Osum, Devoll, Shkumbin, Erzen, Mat and Drin rivers (Figure 1) and all of them are less than 272 km long.

Fluvial terrace deposition punctuates the vertical incision along all the main Albanian rivers (Figure 2) and most of them are located above soft clastic (flysch or molasses) sediments. The terraces of the upper Vjosa River (also called Voidomatis in Greece), the middle Vjosa River, the Osum River, the Erzen River and the Drin River were previously mapped and dated by Woodward et al. [2008], Hauer et al. [2021], Carcaillet et al. [2009], Koçi [2007] and by Gemignani et al. [2022], respectively. We performed an analysis of the terrace geometry and new dating for the Devoll, Skumbin, Mat and Erzen rivers, previously poorly studied. The lower part of the Drin River has not been studied because it is drowned by several artificial dams.

4. Terrace geomorphology and ages along the seven Albanian rivers

A synthesis of the numerical dating and terrace geometry is presented for the rivers of Albania and northwestern Greece. A nomenclature is proposed, where the successions of terraces surface for each river are called $Tx_{(river)}$ and terrace indices increase with age. Units are nonetheless labelled $Ux_{(river)}$ when the terrace surface, fully eroded, cannot be defined. A correlation of this nomenclature with those used by the previous terrace studies is shown in

Table 3 and detailed in Supplementary Information, Appendix 3.

4.1. *Previous studies of the Vjosa, Drin and Osum river terraces*

The Vjosa River is more than 272 km long and is made up of sections with very different morphologies [Hauer et al., 2021].

In the upper section (Konista area, Figure 1), eight units (Figure 4a), including the present-day channel ($T1_{(vj)}$), were identified. They were dated, except $T2_{(vj)}$, using different methods (^{14}C, U/Th, ESR, TL) [Lewin et al., 1991, Hamlin et al., 2000, Woodward et al., 2001, 2008] (Table 2). The highest terrace was deposited by a river system with a much larger catchment that was pirated before 350 ka [Macklin et al., 1997].

In the middle section of the Vjosa River, the long-term incision rate is greater than in the upper section [Guzmán et al., 2013]. The elevation of the highest terrace $T10_{(vj)}$ (Figure 3a) is more than 160 m [Prifti, 1981] and our field work has shown that the conglomerate unit of $T10_{(vj)}$ is preserved between paleo-meanders filled by sediment of $T9_{(vj)}$. Prifti and Meçaj [1987] mapped five terrace levels and Guzmán et al. [2013] mapped another terrace level $T2_{(vj)}$ that is located at the top of a thick sedimentary unit that extends several tens of meters below the present river [Prifti, 1981].

The units beneath the terrace surfaces are mainly formed of rounded fluvial clasts. Nonetheless, angular calcareous clasts are locally intercalated within the fluvial units and are related to debris flows (Figure 3b) provided by very steep calcareous slopes. Guzmán et al. [2013] dated colluvium above the top of $T2_{(vj)}$.

We dated in this paper $T5_{(vj)}$ with an age intercalated between those found in the upper section for $T4_{(vj)}$ and $T6_{(vj)}$ [Woodward et al., 2008]. Hence, when the upper and middle sections of the Vjosa River are considered, ten river terrace levels are identified and only $T9_{(vj)}$ is not dated (Figure 3a, Table 2).

Along the Drin River, four terraces are described [Aliaj et al., 1996, Pashko and Aliaj, 2020]. Our personal work close to Peshkopia area (Figure 1) has revealed two others higher terraces, $T5_{(dr)}$ and $T6_{(dr)}$ (Figure 3f). Only $T2_{(dr)}$ and $T3_{(dr)}$ terraces were dated [Gemignani et al., 2022] (Table 2).

In the Osum River area, nine terraces were mapped [Carcaillet et al., 2009] and our complementary observations indicate remnants of a fill terrace ($T10_{(os)}$) more than 150 m above the present-day river (Figure 3b). The sedimentary unit linked to $T4_{(os)}$ is superimposed above another allostatigraphic unit $U5_{(os)}$ in the middle reaches of the Osum River [Carcaillet et al., 2009]. Using ^{14}C and ^{10}Be dating methods, Carcaillet et al. [2009] dated $T7_{(os)}$, $T6_{(os)}$, $T3_{(os)}$, and $T2_{(os)}$ and also $U5_{(os)}$ (Table 2).

4.2. *New results about the paleo-Devoll, Mat and Erzen terraces*

4.2.1. *A paleo-Devoll River defined from the Devoll and Shkumbin terraces*

The Devoll River flows over 205 km. Downstream from the confluence with the Osum River, it forms the Seman River (Figure 5a).

The Shkumbin River is 181 km long and the Devoll and Shkumbin are two nearby rivers that are presently separated by the Cërrik plain spanning approximately 20 km^2. Today, no river flows through this plain (Figure 5a) that dips ~0.1° toward the northwest but terraces of a paleo-river are perched above its eastern border. The Cërrik plain is located over a thick sedimentary unit [Prifti and Meçaj, 1987] and the scarp cut by the Devoll River shows a >12 m-thick deposit formed of pebbles supported by a sandy to silty matrix. Our measurements of imbricate clasts and cross stratification indicate paleoflow directions around N 300° and N 340° during deposition (site 1 and 2 on Figure 4c and Supplementary Information, Appendix 4). This suggests that the paleo-Devoll River flowed northward and connected to the Shkumbin River. Hence, the terraces located along the middle reaches of the Devoll and the lower reaches of the Shkumbin form a unique terrace system that extends more than 100 km.

Four and six terrace levels were initially identified along the Shkumbin [Melo, 1961] and Devoll [Prifti, 1984] rivers, respectively. In this study (Supplementary Information, Appendix 5), we mapped and correlated eleven terrace levels along the paleo-Devoll River (Table 3 and Figure 3c). Their sedimentary units were generally deposited on straths beveled in the flysch or molasse substratum.

The mean thickness of $T12_{(pa)}$, $T11_{(pa)}$, $T9_{(pa)}$, $T8_{(pa)}$, $T7_{(pa)}$, $pT6_{(pa)}$, and $T5_{(pa)}$, $T4_{(pa)}$ and $T3_{(pa)}$

Table 3. Correlation of the local terrace nomenclatures with a regional nomenclature for the terraces identified along the Albanian rivers

River	Vjosa – Middle section	Vjosa – Upper section		Osum		Paleo-Devoll			Erzen		Mat		Drin		Regional nomenclature	Regional abandonment ages (ka)
Author	Prifti and Meçaj [1987], Guzmán et al. [2013]	Woodward et al. [2008]	This study	Carcaillet et al. [2009]	This study	Melo [1961] - Shkumbin river	Prifti [1984] Devoll river	This study	Koçi et al. [2018]	This study	Melo [1996]	This study	Gemignani et al. [2022]	This study		
Terrace	T_V (P & M)	U8	$T10_{(vj)}$		$T10_{(os)}$			$T12_{(pa)}$		-		-		$T6_{(dr)}$	T12	>350?
			$T9_{(vj)}$	T1	$T9_{(os)}$		T_{VI}	$T11_{(pa)}$		-	T_V	$T9_{(ma)}$		$T5_{(dr)}$	T11	>193
								$U10_{(pa)}$							$U10_{(pa)}$	
	T_{IV} (P & M)	U7	$T8_{(vj)}$	T2	$T8_{(os)}$	T_{IV}	T_V	$T9_{(pa)}$	T1	$T7_{(er)}$	T_{IV}	$T8_{(ma)}$			T10	90–117
	T_{III} (P & M)	U6	$T7_{(vj)}$	-	-			-		-	T_{III}	$T7_{(ma)}$		-	T9	68–87
	T_{II} (P & M)	U5	$T6_{(vj)}$	T3	$T7_{(os)}$	T_{III}	T_{IV}	$T8_{(pa)}$	T2	$T6_{(er)}$		$T6_{(ma)}$		-	T8	52 (−2/+3)
			-	T4	$T6_{(os)}$			$T7_{(pa)}$				-		-	T7	42 (−0.5/+1.5)
			-	T5	$pT5_{(os)}$			$pT6_{(pa)}$	T3	$T5_{(er)}$	T_{II}	$T5_{(ma)}$		-	T6	35.5 (−1/+2)
	T_I (P & M)		$T5_{(vj)}$	T6	$T4_{(os)}$	T_{II}	T_{III}	$T5_{(pa)}$		$T4_{(er)}$		-		-	T5	29.5 (±1)
		U4	$T4_{(vj)}$		-			$T4_{(pa)}$		-	T_I	$T4_{(ma)}$		-	T4	25 (−2/+1)
		U3	$T3_{(vj)}$	T7	$T3_{(os)}$		T_{II}	$T3_{(pa)}$		-		$T3_{(ma)}$	T3	$T4_{(dr)}$	T3	16.5–22
			-	T8	$T2_{(os)}$	T_I	T_I	-		-		-	T2	$T3_{(dr)}$	T2	11–12
	T1 (G & al.)	U2	$T2_{(vj)}$		-			$T2_{(pa)}$	T4	$T3_{(er)}$		$T2_{(ma)}$	T1	$T2_{(dr)}$	T1	5.7–6.3; 7.6–10
		U1-actual	$T1_{(vj)}$	T9	$T1_{(os)}$			$T1_{(pa)}$	T5	$T2_{(er)}$		$T1_{(ma)}$		$T1_{(dr)}$	T0	0.2–1
									T6	$T1_{(er)}$					T0	0–0.2

The light green cells refer to dated levels; light yellow and white cells refer to not dated levels, well correlated or poorly correlated, respectively. The colored cells on the right side refer to the color code of Figures 3, 5, 7 and 9. The regional ages of the terrace and their uncertainties (68% probability interval) are obtained from the probability density curves of the numerical dating for terraces younger than 60 ka (see text and Figure 9). "P & M" stands for Prifti and Meçaj [1987] and "G and al." stands for Guzmán et al. [2013].

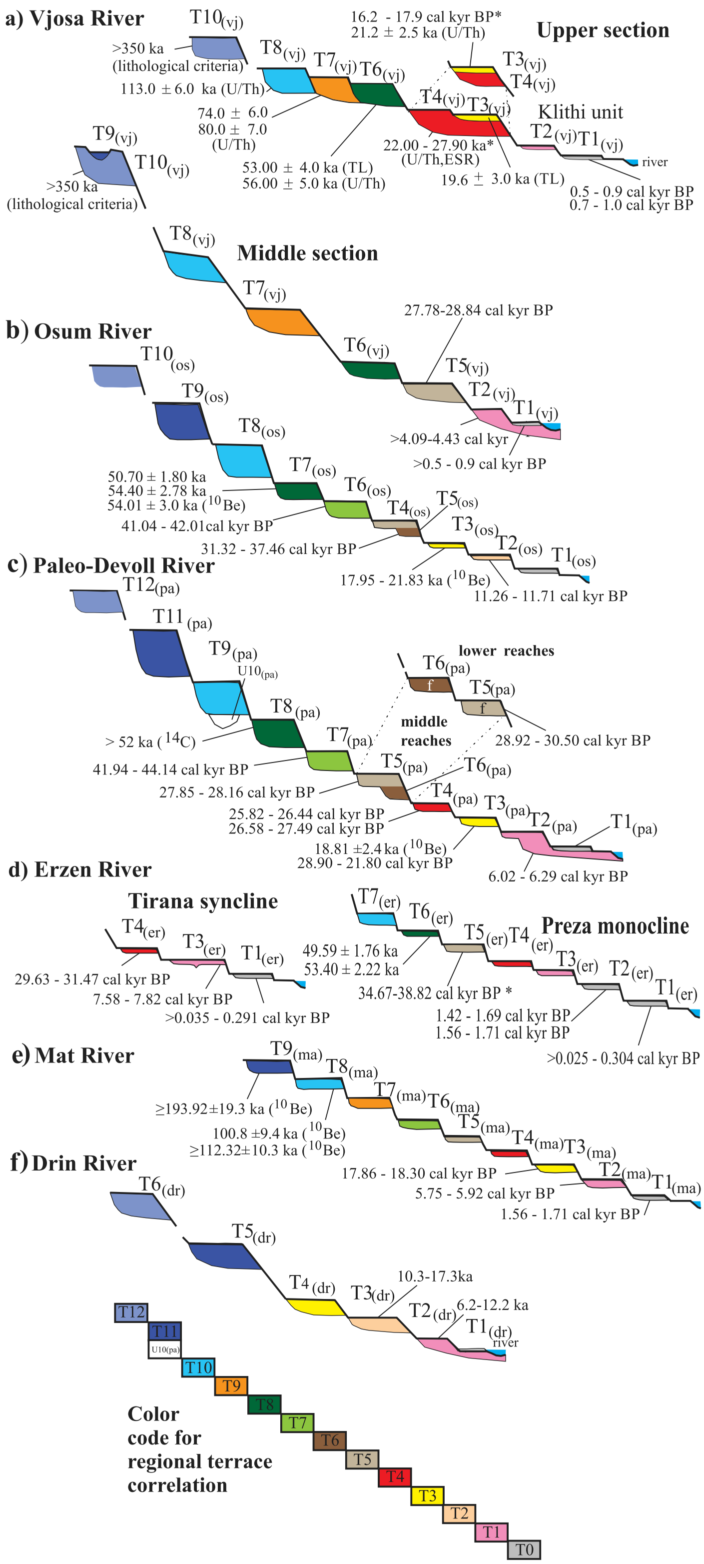

Figure 3. Caption continued on next page.

Figure 3. (**cont.**) Ages and simplified geometry of the terraces identified along the 7 main Albanian rivers (a–f; see text). The horizontal and vertical axes are not to scale. The local terrace nomenclature $TX_{(loc)}$ is indicated for each river. The color of the terraces indicates the inferred correlation with the regional nomenclature T0 to T12 (Same colors as cells of Table 3). The ages refer to the numerical ages of Table 2. Ages are shown as a unique interval with an "*" if there are three or more numeric dates for one terrace level.

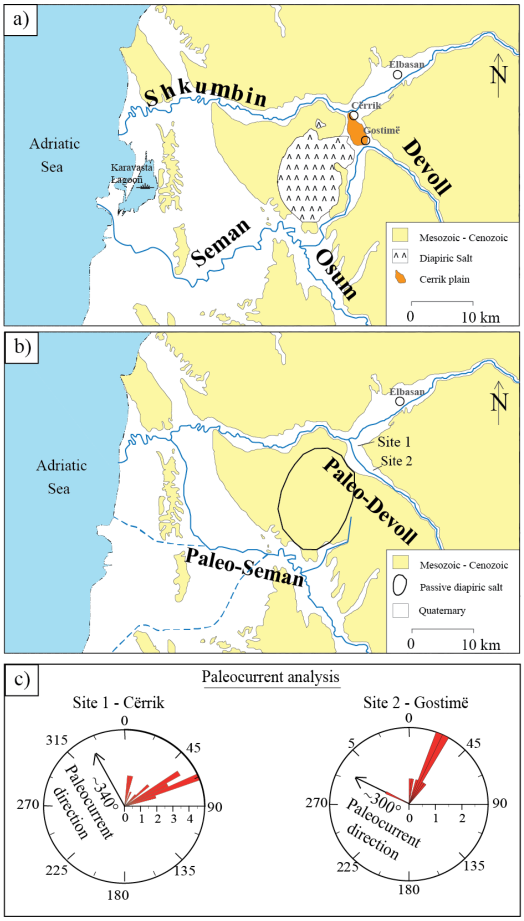

Figure 4. Evolution of the connections between the Devoll, Osum, Seman and Shkumbin rivers. (a) Present-day configuration. (b) Previous configurations. The age of the capture of the Devoll by the Seman is estimated at 6 ka (see text). The paleo-Seman River from Chabreyrou [2006, full line] and Fouache et al. [2010, dashed lines]. (c) Rose diagrams of the paleo-flow directions inferred from imbricate clasts and cross stratification. Location of sites 1 and 2 on Figure 4b (data in the Supplementary Information, Appendix 4).

vary between 6 and 32 m and two superposed sub-units, that are part of parts of the same fluvial process, are found beneath all these terraces: A thin upper sedimentary sub-unit (~1 m) is composed of clay, siltstone and fine sand. Nevertheless, its thickness reaches more than 2 m beneath the oldest terraces ($T12_{(pa)}$, $T11_{(pa)}$ and $T9_{(pa)}$) and possibly includes loess and colluvium deposited after the fluvial story. The basal sub-unit consists of rounded pebbles and cobbles that are supported by a gravel and sand matrix. The clast size generally fines upward, while the percentage of matrix increases. Nonetheless, the size of the coarse material shows complex variations and conglomerate sometimes alternate with horizontal stratified, fine to coarse sand levels. Sediments of the basal unit were deposited in a braided alluvial system characterized by cross-stratified rounded pebbles and cobble levels that alternate with horizontal stratified, fine to coarse sand levels.

The upper part of $T10_{(pa)}$ is fully eroded and $U10_{(pa)}$ is only found beneath an erosional surface in the continuity of the strath at the bottom of $T9_{(pa)}$. Evidence of a meandering environment is found within the unit $U10_{(pa)}$ (Figure 3c) where sediments dip steeply and were possibly deposited at the intrados of meanders.

In the lower reaches of the paleo-Devoll catchment, a cosmogenic depth profile (Figure 8a) yielded a minimum exposure age for $T3_{(pa)}$ (Table 1; see the description in Supplementary Information, Appendix 2) and seven ^{14}C samples were collected along the paleo-Devoll River (Table 2). These results, combined with the eleven ^{14}C dates [Guzmán et al., 2013] gave ages for $T8_{(pa)}$, $T7_{(pa)}$, $T5_{(pa)}$, $T4_{(pa)}$, $T3_{(pa)}$, and $T2_{(pa)}$. Furthermore, the ^{14}C dating of colluvium deposited above $T1_{(pa)}$ provides an age for the abandonment of this terrace.

4.2.2. *Characteristics and numerical ages of the Mat terraces*

Five terraces were previously described along the Mat River [Melo, 1996]. Nine terraces (Figure 3e) were mapped during our fieldwork (Figure 7).

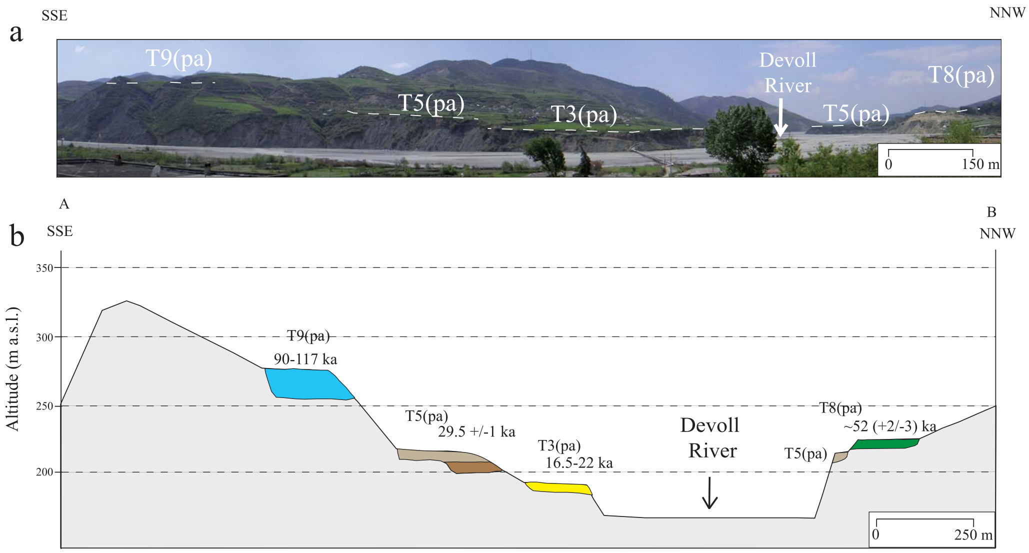

Figure 5. The terraces of the upper reaches of the Devoll River. (a) Panoramic view and (b) cross-section through the terraces. The ages refer to the regional nomenclature and to the most likely age of abandonment proposed in this study (Table 3).

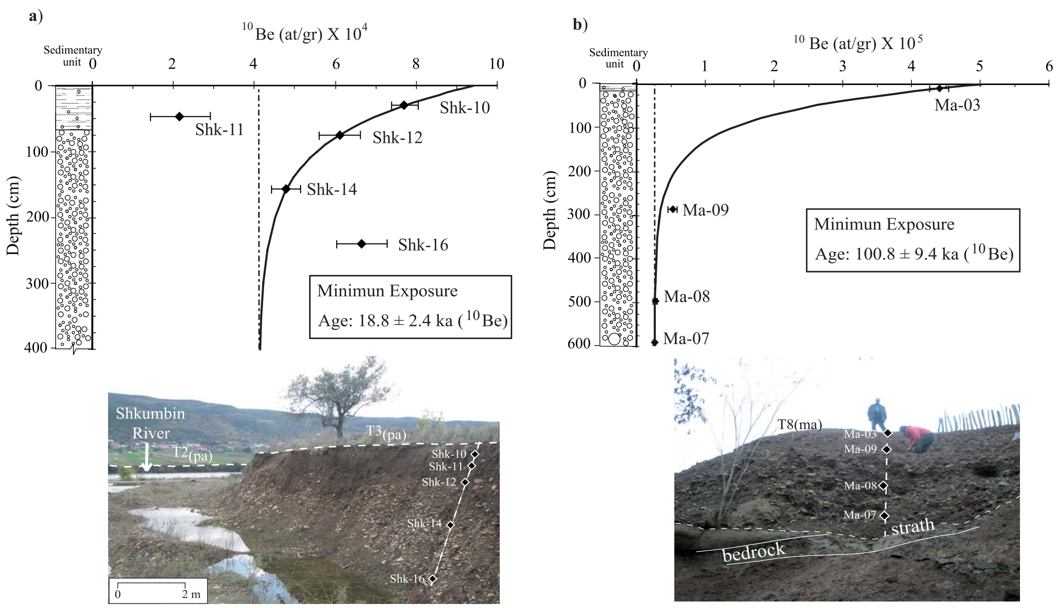

Figure 6. The ^{10}Be concentration along the depth profiles. (a) $T3_{(pa)}$ in the lower reaches of the paleo-Devoll River (location of Sk-10 on the Supplementary Information, Figure S4a in Appendix 5); (b) $T8_{(ma)}$ in the middle reaches of the Mat River (Ulza Dam, location on Figure 7). Solid lines indicate the best-fit for the depth-production profile; the dashed line shows the inherited ^{10}Be concentration. Details are given in Table 1 and in the Supplementary Information, Appendix 2.

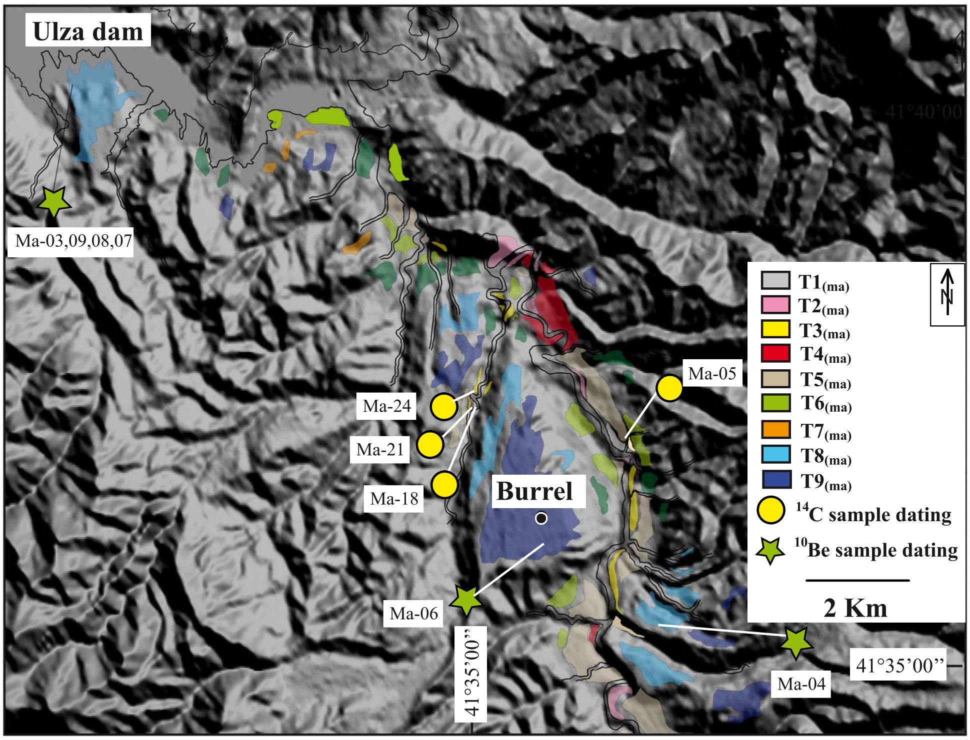

Figure 7. Geomorphologic map of the Mat River. Location on Figure 1. The numbers refer to the samples of Table 2.

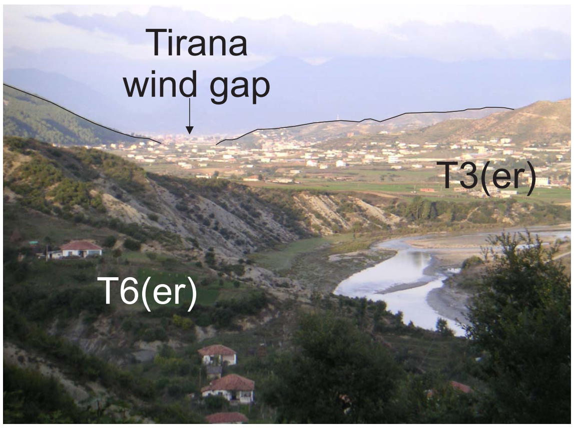

Figure 8. Terraces of the Erzen River. ($T3_{(er)}$) extending toward the Tirana wind gap.

The two oldest terraces were dated using the ^{10}Be method. Amalgams of siliceous pebbles (e.g. radiolarites, chert, quartz), were taken at the top of $T9_{(ma)}$ and $T8_{(ma)}$ (Ma-06 and Ma-04in Table 1; location on Figure 7). A cosmogenic depth profile was made through the sedimentary unit of terrace $T8_{(ma)}$ (Figure 6b). Terraces $T3_{(ma)}$, $T2_{(ma)}$, $T1_{(ma)}$ and the colluvium deposited above $T1_{(ma)}$ were dated from charcoal samples (Table 2 and Figure 3e).

4.2.3. *Characteristics and numerical ages of the Erzen terraces*

The terraces of the Erzen River have been mapped by Koçi [2007] and an active back-thrust fault separates two domains [Ganas et al., 2020]. In the western uplifted domain (Prespa monocline), seven levels of terraces were recognized (Figure 3d) whereas in the eastern domain (Tirana syncline), only three terrace levels were recognized. A correlation between the terraces on each side of the back-thrust fault is made using the 15 ^{14}C dates (Table 2) and seven terrace levels were identified along the Erzen River ($T7_{(er)}$ to $T1_{(er)}$), and only the oldest level is not numerically dated. The terrace $T3_{(er)}$ is highly extended, in peculiar across a wind gap (Figure 8), which corresponds to a paleo river that flowed close to Tirana (Figure 1).

5. Discussion

5.1. *A regional correlation of the Albanian terraces based on numerical ages*

Few samples have been discarded during our work (Table 2): two ^{14}C samples, that furnished less than 200-year ages in old terraces, were considered as related to the reworking of recent organic pieces. The Carbon quantity of five samples was too small (less than 0.12 mg) to give numerical ages. Two ^{10}Be samples were also excluded from the profile interpretations because one was probably transported by a small tributary and the other one affected by a probable chemical problem during the preparation (Supplementary Information, Appendix 2). Finally, two TL ages published by Lewin et al. [1991] were removed due to their very high uncertainty.

Thirty-one out of the 49 local terrace levels ($Tx_{(river)}$, Figure 4) recognized along the seven rivers were dated, providing a solid framework for a regional correlation (Tx) based on the synchronicity of numerical ages. No simple relationship between altitude and age is observed at the scale of Albania (Figure 9a) due to the variable uplift rate in the Albanian mountains [Guzmán et al., 2013].

To consider the 60 numerical ages younger than 60 ka, a regional probability density curve was obtained from the summation of the individual probability distribution ages [Ramsey, 2009], a method already used in terrace chronology studies [e.g. Meyer et al., 1995, Wegmann and Pazzaglia, 2002, 2009]. The summation (Figure 9b) shows time periods where the probability of sedimentation is null and ten high probability peaks. These peaks define the ages of T0 to T8 (Table 3, see details of the correlation in Supplementary Information, Appendix 6).

The ages greater than 60 ka are few in number and the regional T9 to T12 levels are only defined by one or two ages. Eighteen terrace levels are not numerically dated along the various rivers. Their intercalation between dated levels provides a rather good relative age (yellow cells on Table 3) or their elevation relative to the dated terrace levels only provides a poor relative chronology (white cells in Table 3).

5.2. *The influence of the paleoclimate on the genesis of Albanian terraces*

The comparison of the Albanian terraces ages with climatic proxies [Grootes et al., 1993, de Abreu et al., 2003, Wagner et al., 2009, 2010] is a rather difficult exercise given the uncertainties about the terrace abandonment ages (more than one thousand years) and the short-term fluctuations in the climatic records [less than one thousand years, Ziemen et al., 2019]. A robust criterion could be based on models that link the timing of sedimentation and incision with the temperature, hydrology and vegetation evolutions during a climatic cycle [Bull, 1991].

Cold periods in Albania are associated with less precipitation [Kallel et al., 2000, Toucanne et al., 2015] and we consider the classic model for these climatic contexts, where vertical incision is favored by the increase of the transport capacity that occurs at the transition from cold and dry conditions to warmer and more humid conditions [e.g. Fuller et al., 1998, Bridgland and Westaway, 2008]. This model has been proposed to define the "cold" terraces in the lowlands of northern Europe [Vandenberghe, 2015], to correlate terraces at the Mediterranean scale [Macklin et al., 2002], to interpret terraces in semi-arid conditions [Vassallo et al., 2007] and to interpret the nested terraces in Northern Apeninnes [Wegmann and Pazzaglia, 2009] or the western Carpathians [Olszak, 2017].

The succession of cold periods followed by rapid warm excursions, could effectively cause the abandonment of most terraces (Figure 9c): T2, T6 and T7 are synchronous with the end of the Younger Dryas, the Dansgaard-Oeschger events number 7 and 11, respectively [Dansgaard et al., 1993, North Greenland Ice Core Project Members, 2004]. Furthermore, the abandonments of T8, T5, T4, and T3 (Figure 9b) correlate rather well with the H5a [Rashid et al., 2003], H3, H2, and H1 Heinrich events [Hemming, 2004], respectively (Figure 9c). These Heinrich events were already recorded in this area [Wagner et al., 2009, 2010] (gray rectangle on Figure 9d–f).

The ranges of the terrace ages, defined by the 95% probability interval of the summation curve, therefore include the ages of transitions between cold-dry and warm-wet periods. Nonetheless, as the climatic transitions were dated more precisely than the Albanian terraces (less than a thousand years vs. more

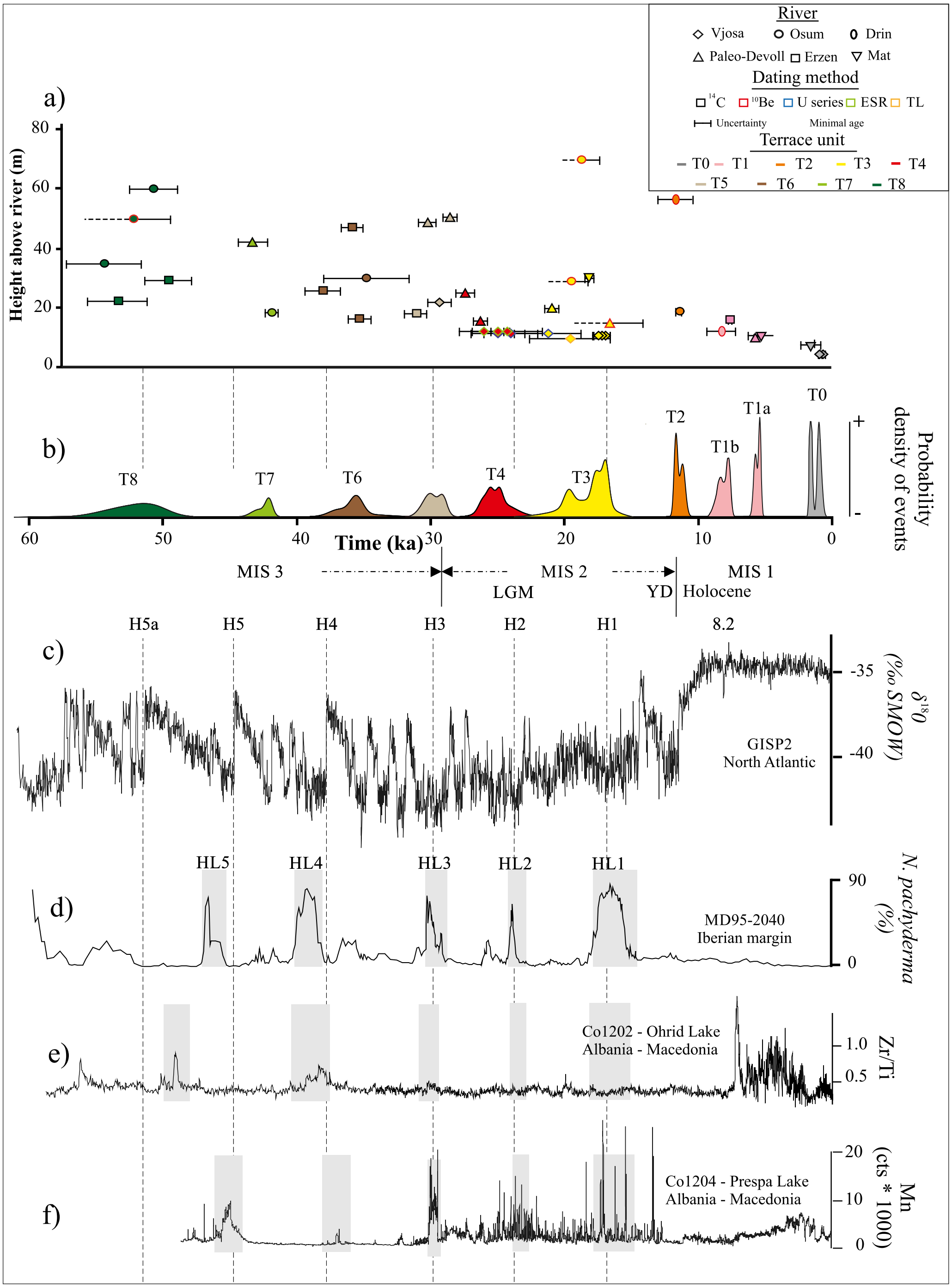

Figure 9. Caption continued on next page.

Figure 9. (**cont.**) Compilation of the Albanian terrace ages for the last 60 ka (Table 2) and comparison with climatic proxis. (a) Plot of individual ages and their two sigma (95%) probability. Each terrace is represented by a symbol, a contour color and a fill color corresponding to the river, the dating method and the terrace level (regional nomenclature), respectively. The horizontal axis is the terrace age while the vertical axis is the height of the terrace above the present-day river. (b) The regional probability density curve produced by summing the probability distribution of the individual ages; (c) The δ^{18}O record from the GISP2 ice core [Grootes et al., 1993]. (d) The percentage of the cold-water foraminifera N. pachyderma from the Iberian margin [de Abreu et al., 2003]. (e) The paleo-environmental record from Lake Ohrid (Zirconium/Titanium ratio: Zi/Ti) [Wagner et al., 2009]; and (f) the paleo-environmental record from Lake Prespa (Manganese: Mn) [Wagner et al., 2010]. The timings of the Heinrich events (H1 to H5a) are taken from Rashid et al. [2003] and Hemming [2004]. The gray rectangles represent the Heinrich events as identified by the authors of curves (d–f). MIS, LGM and YD stand for Marine Isotope Stage [Cacho et al., 1999], Last Glacial Maximum [Clark et al., 2009] and Younger Dryas [Berger, 1990], respectively.

than a thousand years), our results do not prove the "cold" terrace model of Vandenberghe [2008] and are only in agreement with this model of terrace genesis.

However, while rapid changes during the glacial cycle, such as DO or HE events, can induce the formation of "cold" terraces, the major changes that occur between the glacial and interglacial periods are not generally considered in this model. This is the case of T1 that is not synchronous with a cold to warm transition. Vandenberghe [2008] suggests that, in addition to the "cold" terrace model, deep channels may be very rapidly incised and then filled at the beginning of a warm period. This results in a "warm" unit model [Vandenberghe, 2008] and situations of rivers leaving their valley to take another course [Vandenberghe, 1993] frequently typify "warm" units [Vandenberghe, 2015].

T1 is related to the Holocene climatic optimum and a great aggradation along the Vjoje (Figure 3a) as well as deviations of the rivers at the Cërrik and the Tirana wind gaps (Figure 4 and Figure 8) were recorded during this period. The T1 terrace would therefore be in line with the "warm" unit model [Vandenberghe, 2015]. Similarly, the $U10_{(pa)}$, remnant of a valley fill older than the T10 (90–117 ka) overlying unit, may have been deposited during the Eemian interglacial (MIS-5e) stage and could be a "warm" sedimentary unit [Vandenberghe, 2015].

6. Conclusions

Geomorphologic studies and new dating have been performed along the Devoll, Shkumbin, Mat and Erzen rivers of Albania (30 ^{14}C sites, two ^{10}Be profiles and two ^{10}Be surface sites). A comparison is also made with previous studies along the Vjosa, Osum and Drin rivers. This work has led to a database of 70 ages and a time correlation has been performed between the flights of terraces observed along the seven rivers. It appears that 11 terrace levels have been preserved during the last 200 ka in Albania and this record contains most of the major phases of terrace formation in the Mediterranean region during the last glacial cycle. The exceptional preservation of the succession of Albanian terraces is probably due to the combination of a moderate uplift rate (0.5 to 1 mm/year) and a medium strength of the bedrock lithology (mainly flysch or molasse) specific to this area. During the Holocene, T1 terrace level was recognized, along with the capture of the Devoll River by the Osum River and a tributary deviation away from the Erzen. Eight terraces (T2 to T10) were identified and dated during the last glacial period (MIS 5d to end of MIS 2). For the older periods, amongst the numerous observed terrace remnants, only a unique of T11 was dated at $\geq 194 \pm 19$ ka (MIS 6).

The abandonment of the Albanian terrace surfaces was mainly controlled by climatic variations and was generally synchronous with the interstadial transitions during the last glacial period. This indicates that the threshold necessary for a cold to warmer climatic control for terrace development is reached during interstadial climatic events as short as Heinrich events.

Declaration of interests

The authors do not work for, advise, own shares in, or receive funds from any organization that could benefit from this article, and have declared no affiliations other than their research organizations.

Acknowledgements

The authors would like to thank the NATO SFP 977993 and the Science for Peace team for supporting this work. OG thanks the Simon Bolivar University for granting him permission to carry out his doctoral studies. This publication was also made possible through a grant provided by the Institut de Recherche et Developement. We warmly thank the staff of the AMS facility ASTER at the Centre Européen de Recherche et d'Enseignement des Géosciences de l'Environnement (CNRS, France) for technical assistance during the ^{10}Be measurements. We thank one anonymous reviewer and Johannes Preuss for helpful comments.

Supplementary data

Supporting information for this article is available on the journal's website under https://doi.org/10.5802/crgeos.251 or from the author.

References

Aliaj, S., Melo, V., Hyseni, A., Skrami, J., Mëhillka, L., Muço, B., Sulstarova, E., Prifti, K., Pashko, P., and Prillo, S. (1996). *Neo-tectonic Map of Albania in Scale 1:200000*. Archive of Seismology Institute, Tirana, Albania. (In Albanian).

Antoine, P., Moncel, M.-H., Limondin-Lozouet, N., Locht, J., Bahain, J., Moreno, D., Voinchet, P., Auguste, P., Stoetzel, E., Dabkowski, J., Bello, S., Parfitt, S., Tombret, O., and Hardy, B. (2016). Palaeoenvironment and dating of the Early Acheulean localities from the Somme River basin (Northern France): New discoveries from the High Terrace at Abbeville-Carrière Carpentier. *Quat. Sci. Rev.*, 149, 338–371. https://www.sciencedirect.com/science/article/abs/pii/S0277379116302700.

Bard, E., Rostek, F., and Ménot-Combes, G. (2004). Radiocarbon calibration beyond 20,000 ^{14}C yr BP by means of planktonic foraminifera of the Iberian Margin. *Quat. Res.*, 61, 204–214. https://www.sciencedirect.com/science/article/abs/pii/S0033589403001698.

Berger, W. H. (1990). The Younger Dryas cold spell—a quest for causes. *Glob. Planet. Change*, 3(3), 219–237. https://www.sciencedirect.com/science/article/abs/pii/0921818190900188.

Biermanns, P., Schmitz, B., Ustaszewski, K., and Reicherter, K. (2018). Tectonic geomorphology and Quaternary landscape development in the Albania—Montenegro border region: An inventory. *Geomorphology*, 326, 116–131.

Bond, G., Heinrich, H., Broecker, W., Labeyrie, L., Mcmanus, J., Andrews, J., Huon, S., Jantschik, R., Clasen, S., and Simet, C. (1992). Evidence for massive discharges of icebergs into the North Atlantic Ocean during the last glacial period. *Nature*, 360, 245–249. https://www.nature.com/articles/360245a0.

Bridgland, D. and Westaway, R. (2008). Climatically controlled river terrace staircases: A worldwide Quaternary phenomenon. *Geomorphology*, 98, 285–315. https://www.sciencedirect.com/science/article/abs/pii/S0169555X0700236X.

Bull, W. B. (1991). *Geomorphic Responses to Climate Change*. Oxford University Press, Oxford, https://www.osti.gov/biblio/5603696.

Cacho, I., Grimalt, J. O., Pelejero, C., Canals, M., Sierro, F. J., Flores, J. A., and Shackleton, N. J. (1999). Dansgaard–Oeschger and Heinrich event imprints in Alboran Sea paleotemperatures. *Paleoceanography*, 14, 698–705. https://www.semanticscholar.org/paper/Dansgaard%E2%80%90Oeschger-and-Heinrich-event-imprints-in-Cacho-Grimalt/a2dda1e4955c28de37c151ae3f0a1fa3400b3ff8.

Carcaillet, J., Mugnier, J. L., Koçi, R., and Jouanne, F. (2009). Uplift and active tectonics of southern Albania inferred from incision of alluvial terraces. *Quat. Res.*, 71, 465–476. https://www.sciencedirect.com/science/article/abs/pii/S0033589409000039.

Chabreyrou, J. (2006). *Morphologie fluviale et structures tectoniques actives en Albanie*. Masters thesis, Université Joseph Fourier, France.

Chappell, J. (2002). Sea level changes forced ice breakouts in the Last Glacial cycle: new results from coral terraces. *Quat. Sci. Rev.*, 21, 1229–1240. https://www.sciencedirect.com/science/article/abs/pii/S027737910100141X.

Clark, P. U., Dyke, A. S., Shakun, J. D., Carlson, A. E., Clark, J., Wohlfarth, B., Mitrovica, J. X., and Hostetler, S. W. (2009). The last glacial maximum.

Science, 325, 710–714. https://www.science.org/doi/10.1126/science.1172873.

Clement, A. C. and Peterson, L. C. (2008). Mechanisms of abrupt climate change of the last glacial period. *Rev. Geophys.*, 46, article no. RG4002.

Cordier, S., Briant, B., Bridgland, D., Herget, J., Maddy, D., Mather, A., and Vandenberghe, J. (2017). The Fluvial Archives Group: 20 years of research connecting fluvial geomorphology and palaeoenvironments. *Quat. Sci. Rev.*, 166, 1–9. https://www.sciencedirect.com/science/article/abs/pii/S0277379117301944.

Cremaschi, M., Zerboni, A., Nicosia, C., Negrino, F., Rodnight, H., and Spötl, C. (2015). Age, soil-forming processes, and archaeology of the loess deposits at the Apennine margin of the Po plain (northern Italy): New insights from the Ghiardo area. *Quat. Int.*, 376, 173–188. https://www.sciencedirect.com/science/article/abs/pii/S1040618214005138.

Dansgaard, W., Johnsen, S. J., Clausen, H. B., Dahl-Jensen, D., Gundestrup, N. S., Hammer, C. U., Hvidberg, C. S., Steffensen, J. P., Sveinbjörnsdottir, A. E., Jouzel, J., and Bond, G. (1993). Evidence for general instability of past climate from a 250,000- year ice-core record. *Nature*, 364, 218–220. https://www.nature.com/articles/364218a0.

de Abreu, L., Shackleton, N. J., Schönfeld, J., Hall, M. A., and Chapman, M. R. (2003). Millennial-scale oceanic climate variability off the Western Iberian margin during the last two glacial periods. *Mar. Geol.*, 196, 1–20. https://www.sciencedirect.com/science/article/abs/pii/S002532270300046X.

Fouache, E., Vella, C., Dimo, L., Gruda, G., Mugnier, J.-L., Denefle, M., Monnier, O., Hotyat, M., and Huth, E. (2010). Shoreline reconstruction since the Middle Holocene in the vicinityof the ancient city of Apollonia (Albania, Seman and Vjosa deltas). *Quat. Int.*, 216, 118–128.

Fuller, I. C., Macklin, M. G., Lewin, J., Passmore, D. G., and Wintle, A. G. (1998). River response to high-frequency climate oscillations in southern Europe over the Past 200 k.y. *Geology*, 26, 275–278. https://www.researchgate.net/publication/249520546_River_response_to_high-frequency_climate_oscillations_in_southern_Europe_over_the_past_200_ky.

Ganas, A., Elias, P., Briole, P., Cannavo, F., Valkaniotis, S., Tsironi, V., and Partheniou, E. (2020). Ground deformation and seismic fault model of the M6.4 Durres (Albania) Nov. 26, 2019 earthquake, based on NSS/INSAR observations. *Geosciences*, 10, article no. 210.

Gemignani, L., Mittelbach, B., Simon, D., Rohrmann, A., Grund, M., Bernhardt, A., Hippe, K., Giese, J., and Handy, M. (2022). Response of drainage pattern and basin evolution to tectonic and climatic changes along the Dinarides-Hellenides orogen. *Front. Earth Sci.*, 10, article no. 821707.

Geraga, M., Tsaila-Monopolis, S., Ioakim, C., Papatheodorou, G., and Ferentinos, G. (2005). Short-term changes in the southern Aegean Sea over the last 48,000 years. *Palaeoceanor. Palaeoclimatol. Palaeoecol.*, 220, 311–332. https://www.sciencedirect.com/science/article/abs/pii/S0031018205000428.

Gosse, J. and Phillips, F. (2001). Terrestrial *in situ* cosmogenic nuclides: theory and application. *Quat. Sci. Rev.*, 20, 1475–1560. https://www.sciencedirect.com/science/article/abs/pii/S0277379100001712.

Grootes, P. M., Stuiver, M., White, J., Johnson, S., and Jouzel, J. (1993). Comparison of oxygen isotope records from the GISP2 and GRIP Greenland ice cores. *Nature*, 366, 552–554. https://www.nature.com/articles/366552a0.

Guzmán, O., Mugnier, J. L., Vassallo, R., Koçi, R., and Jouanne, F. (2013). Vertical slip rate of major active faults of southern Albania inferred from river terraces. *Ann. Geophys. Earthquake Geol.*, 56, 1–17.

Hamlin, R., Woodward, J., Black, S., and Macklin, M. G. (2000). Sediment fingerprinting as a tool for interpreting long-term river activity: the Voidomatis basin, NW Greece. In Foster, I. D. L., editor, *Tracers in Geomorphology*, pages 473–501. Wiley, Chichester, https://pure.manchester.ac.uk/ws/files/32295226/FULL_TEXT.PDF.

Hauer, C., Skrame, K., and Fuhrmann, M. (2021). Hydromorphologial assessment of the Vjosa river at the catchment scale linking glacial history and fluvial processes. *Catena*, 207, article no. 105598.

Heinrich, H. (1988). Origin and consequences of cyclic ice rafting in the Northeast Atlantic Ocean during the past 130,000 years. *Quat. Res.*, 29, 142–152.

Hemming, S. R. (2004). Heinrich events: Massive Late Pleistocene detritus layers of the North Atlantic and their global climate imprint. *Rev. Geophys.*, 42, article no. RG1005.

Hidy, A. J., Gosse, J. C., Pederson, J. L., Mattern, J. P., and Finkel, R. C. (2010). A geologically constrained Monte Carlo approach to modeling exposure ages from profiles of cosmogenic nuclides: an example from Lees Ferry, Arizona. *Geochem. Geophys. Geosyst.*, 11, 1–18. https://agupubs.onlinelibrary.wiley.com/doi/pdfdirect/10.1029/2010GC003084.

Hughes, P. D. (2010). Geomorphology and Quaternary stratigraphy: The roles of morpho-, litho-, and allostratigraphy. *Geomorphology*, 123, 189–199.

Institutin Topografik te Ushtrise Tirana (1990). *Topographic Maps of Socialist Republic of Albania in Scale: 1:25000*. Archive of Institute of Seismology, Tirana, Albania. (in Albanian).

Kallel, N., Duplessy, J. C., Labeyrie, L., Fontugne, M., Paterne, M., and Montacer, M. (2000). Mediterranean pluvial periods and Sapropel formation over the last 200,000 years. *Palaeogeogr. Palaeoclimatol. Palaeoecol.*, 157, 45–58.

Kallel, N., Paterne, M., Labeyrie, L. D., Duplessy, J. C., and Arnold, M. (1997). Temperature and salinity records of the Tyrrhenian sea during the last 18000 years. *Palaeogeogr. Palaeoclimatol. Palaeoecol.*, 135, 97–108.

Koçi, R. (2007). *Geomorphology of Quaternary deposits of Albanian rivers.* Ph.d. thesis, Archive of Institute of Seismology, Tirana, Albania. (in Albanian language) 217 p.

Koçi, R., Dushi, E., Begu, E., and Bozo, R. (2018). Impact of tectonics on rivers terraces geomorphology in Albania. In *Proceedings of the International Multidisciplinary Scientific GeoConference SGEM*, pages 189–196.

Konijnendijk, T. Y. M., Ziegler, M., and Lourens, L. J. (2015). On the timing and forcing mechanisms of late Pleistocene glacial terminations: insights from a new high-resolution benthic stable oxygen isotope record of the eastern Mediterranean. *Quat. Sci. Rev.*, 129, 308–320.

Lambeck, K. and Chappell, J. (2001). Sea-level change through the last glacial cycle. *Science*, 292, 679–686.

Lewin, J., Macklin, M. G., and Woodward, J. C. (1991). Late Quaternary fluvial sedimentation in the Voidomatis Basin, Epirus, Northwest Greece. *Quat. Res.*, 35, 103–115.

Macklin, M. G., Fuller, I. C., Lewin, J., Maas, G. S., Passmore, D. G., Rose, J., Woodward, J. C., Black, S., Hamlin, R. H. B., and Rowa, J. S. (2002). Correlation of fluvial sequences in the Mediterranean Basin over last 200 ka and their relationship to climate change. *Quat. Sci. Rev.*, 21, 1633–1641.

Macklin, M. G., Lewin, J., and Woodward, J. C. (1997). Quaternary river sedimentary sequences of the Voidomatis Basin. In Bailey, G. N., editor, *Klithi: Palaeolithic Settlement and Quaternary Landscapes in Northwest Greece*, volume 2 of *Klithi in its Local and Regional Setting*, pages 347–359. McDonald Institute for Archaeological Research, Cambridge, https://pure.manchester.ac.uk/ws/portalfiles/portal/32298402/FULL_TEXT.PDF.

Melo, V. (1961). Evidence of neotectonics movements in the Shkumbini terraces along the Elbasani-Peqini sector. State University of Tirana. *Bull. Nat. Sci.*, II, 135–148.

Melo, V. (1996). The terraces of the Mat River. In Aliaj, Sh., Melo, V., Hyseni, A., Skrami, J., Mëhillka, L., Muço, B., Sulstarova, E., Prifti, K., Pashko, P., and Prillo, S., editors, *Neo-tectonic Map of Albania in Scale 1:200000*. Archive of Seismology Institute, Tirana, Albania. (in Albanian).

Meyer, G. A., Wells, S. G., and Jull, A. J. T. (1995). Fire and alluvial chronology in Yellowstone National Park: Climate and intrinsic controls on Holocene geomorphic processes. *Geol. Soc. Am. Bull.*, 107, 1211–1230.

Noller, J. S., Sowers, J. M., and Lettis, W. R. (2000). *Quaternary Geochronology: Methods and Applications*, volume 4. American Geophysical Union, Washington, DC.

North Greenland Ice Core Project Members (2004). High-resolution record of Northern Hemisphere climate extending into the last interglacial period. *Nature*, 431, 147–151.

Obreht, I., Buggle, B., Catto, N., Markovič, S. B., Bösel, S., Vandenberghe, D. A. G., Hambach, U., Svirčev, Z., Lehmkuhl, F., Basarin, B., Gavrilov, M. B., and Jović, G. (2014). The Late Pleistocene Belotinac section (southern Serbia) at the southern limit of the European loess belt: Environmental and climate reconstruction using grain size and stable C and N isotopes. *Quat. Int.*, 334–335, 10–19.

Olszak, J. (2017). Climatically controlled terrace staircases in uplifting mountainous areas. *Glob. Planet. Change*, 156, 13–23.

Ozenda, P. (1975). Sur les étages de végétation dans les montagnes du bassin méditerranéen. *Documents cartographie écologique*, XVI, 1–32. http://ecologie-alpine.ujf-grenoble.fr/articles/DCE_1975_16_1_0.pdf.

Pashko, P. and Aliaj, S. (2020). Stratigraphy and tectonic evolution of late miocene - quaternary basins in Eastern Albania: A review. *Geosociety*, 56, 317–351. https://www.openarchives.gr/aggregator-openarchives/edm/geosociety/000068-geosociety_article_view_22064.

Pazzaglia, F. J. (2022). Fluvial terraces. *Treatise Geomorphol.*, 6, 639–673.

Prifti, K. (1981). Format Kuaternare tëluginës sërrjedhës sësipërme tëVjosës dhe disa veçori karakteristike tëtyre. *Bul. Shk. Gjeol.* Përmbledhje studimesh Nr.2. (In Albanian language).

Prifti, K. (1984). Geomorphology of quaternary deposits of the Devoll River. *Bul. Shk. Gjeol.*, 2, 43–59. (in Albanian).

Prifti, K. and Meçaj, N. (1987). Geomorphologic development of river valleys in Albania and their practice importance. *Geogr. Studies*, 2, 237–253.

Rahmstorf, S. (2002). Ocean circulation and climate during the past 120 000 years. *Nature*, 419, 207–214. https://www.nature.com/articles/nature01090.

Ramsey, B. (2009). Bayesian analysis of radiocarbon dates. *Radiocarbon*, 51, 337–360.

Rashid, H., Hesse, R., and Piper, D. J. (2003). Evidence for an additional Heinrich event between H5 to H6 in the Labrador Sea. *Paleoceanography*, 18, 1077–1091.

Riser, J. (1999). Le Quaternaire. In *Géologie et milieux naturels*, page 320. Dunod, Paris. under the direction of.

Rixhon, G. (2022). A question of time: historical overview and modern thought on quaternary dating methods to produce fluvial chronologies. *Quaternaire*, 33(2).

Robertson, A. and Shallo, M. (2000). Mesozoic-Tertiary tectonic evolution of Albania in its regional Eastern Mediterranean context. *Tectonophys.*, 316, 197–254.

Roucoux, K. H., Tzedakis, P. C., Frogley, M. R., Lawson, I. T., and Preece, R. C. (2008). Vegetation history of the marine isotope stage 7 interglacial complex at Ioannina, NW Greece. *Quat. Sci. Rev.*, 27, 1378–1395.

Roure, F., Nazaj, S., Mushka, K., Fili, I., Cadet, J. P., and Bonneau, M. (2004). Kinematic evolution and petroleum systems - An appraisal of the Outer Albanides. In McClay, K. R., editor, *Thrust Tectonics and Hydrocarbon Systems*, volume 82 of *AAPG Memoir*, pages 474–493. American Association of Petroleum Geologists, Tulsa, Oklahoma.

Rowey, C. and Siemens, M. (2021). Age constraints of the Middle Pleistocene till and loess sequence in northeast Missouri, USA, based on pedostratigraphy within a polygenetic paleosol. *Catena*, 203, article no. 105294.

Sadori, L., Koutsodendris, A., Panagiotopoulos, K., Masi, A., Bertini, A., Combourieu-Nebout, N., Francke, A., Kouli, K., Joannin, S., Mercuri, A.-M., Peyron, O., Torri, P., Wagner, B., Zanchetta, G., Sinopoli, G., and Donders, T. H. (2016). Pollen-based paleoenvironmental and paleoclimatic change at Lake Ohrid (south-eastern Europe) during the past 500 ka. *Biogeosciences*, 13, 1423–1437. https://bg.copernicus.org/articles/13/1423/2016/.

Sánchez Goñi, M. F., Cacho, I., Turon, J.-L., Guiot, J., Sierro, F. J., Peypouquet, J.-P., Grimalt, J. O., and Shackleton, N. J. (2002). Synchroneity between marine and terrestrial responses to millennial scale climatic variability during the last glacial period in the Mediterranean region. *Clim. Dyn.*, 19, 95–105.

Schaller, M., Ehlers, T., Stor, T., Torrent, J., Lobato, L., Christl, C., and Vockenhuber, C. (2016). Timing of European fluvial terrace formation and incision rates constrained by cosmogenic nuclide dating. *Earth Planet. Sci. Lett.*, 451, 221–231.

Schanz, S. A., Montgomery, D. R., Collins, B. D., and Duvall, A. R. (2018). Multiple paths to straths: A review and reassessment of terrace genesis. *Geomorphology*, 312, 12–23. https://www.researchgate.net/publication/324096035_Multiple_paths_to_straths_A_review_and_reassessment_of_terrace_genesis.

Schumm, S. (1979). Geomorphics thresholds: the concepts and its application. *Trans. Inst. Br. Geogr.*, 4, 485–515. http://geomorphology.sese.asu.edu/Papers/Schumm%201979.pdf.

SRTM (2013). NASA Shuttle Radar Topography Mission (SRTM). Distributed by OpenTopography. https://doi.org/10.5069/G9445JDF.

Starkel, L. (1994). Reflection of the Glacial-Interglacial Cycle in the evolution of the Vistula River Basin, Poland. *Terra Nova*, 6, 486–494.

Toucanne, S., Minto'o, C., Fontanier, C., Bassetti, M.-A., Jorry, S., and Jouet, G. (2015). Tracking rainfall in the northern Mediterranean borderlands during sapropel deposition. *Quat. Sci. Rev.*, 129, 178–195.

Tzedakis, P. C., Frogley, M. R., Lawson, I. T., Preece, R. C., Cacho, I., and de Abreu, L. (2004). Ecological thresholds and patterns of millennial-scale climate variability: The response of vegetation in Greece during the last glacial period. *Geology*, 32, 109–112.

Vandenberghe, J. (1993). River Terrace Development and its Relation to Climate: the Saalian Caberg Terrace of the Maas River Near Maastricht (The Netherlands). Mededelingen Rijks Geologische Dienst N.S. 47., 19–24.

Vandenberghe, J. (2003). Climate forcing of fluvial system development: an evolution of ideas. *Quat. Sci. Rev.*, 22, 2053–2060.

Vandenberghe, J. (2008). The fluvial cycle at cold-warm-cold transitions in lowland regions: a refinement of theory. *Geomorphology*, 98, 275–284.

Vandenberghe, J. (2015). River terraces as a response to climatic forcing: Formation processes, sedimentary characteristics and sites for human occupation. *Quat. Int.*, 370, 3–11.

Vassallo, R., Ritz, J.-F., Braucher, R., Jolivet, M., Chauvet, A., Larroque, C., Carretier, S., Bourlès, D., Sue, C., Todbileg, M., Arzhannikova, N., and Arzhannikov, S. (2007). Transpressional tectonics and stream terraces of the Gobi-Altay, Mongolia. *Tectonics*, 26, article no. TC5013.

Wagner, B., Lotter, A. F., Nowaczyk, N., Reed, J. M., Schwalb, A., Sulpizio, R., Valsecchi, V., Wessels, M., and Zanchetta, G. (2009). A 40,000-year record of environmental change from ancient Lake Ohrid (Albania and Macedonia). *J. Paleolimnol.*, 41, 407–430. https://link.springer.com/article/10.1007/s10933-008-9234-2.

Wagner, B., Vogel, H., Zanchetta, G., and Sulpizio, R. (2010). Environmental change within the Balkan region during the past ca. 50 ka recorded in the sediments from lakes Prespa and Ohrid. *Biogesciences*, 7, 3187–3198. https://bg.copernicus.org/articles/7/3187/2010.

Wegmann, K. W. and Pazzaglia, F. J. (2002). Holocene strath terraces, climate change, and active tectonics; the Clearwater River basin, Olympic Peninsula, Washington State. *Geol. Soc. Am. Bull.*, 114(6), 731–744.

Wegmann, K. W. and Pazzaglia, F. J. (2009). Late Quaternary fluvial terraces of the Romagna and Marche Apennines, Italy. *Quat. Sci. Rev.*, 28, 137–165.

Woodward, J. C., Hamlin, R. B. H., Macklin, M. G., Karkanas, P., and Kotjabopoulou, E. (2001). Quantitative sourcing of slackwater deposits at Boila rockshelter: A record of late-glacial flooding and palaeolithic settlement in the Pindus Mountains, Northern Greece. *Geoarchaeology*, 16(5), 501–536.

Woodward, J. C., Hamlin, R. H. B., Macklin, M. G., Hughes, P. D., and Lewin, J. (2008). Glacial activity and catchment dynamics in northwest Greece: Long-term river behaviour and the slackwater sediment record for the last glacial to interglacial transition. *Geomorphology*, 101, 44–67.

Ziemen, F., Kapsch, M.-L., Klockmann, M., and Mikolajewicz, U. (2019). Heinrich events show two-stage climate response in transient glacial simulations. *Clim. Past*, 15, 153–168.